

## Original Article

# Prospective target gene network of key miRNAs influenced by long non-coding RNA HOXA11-AS in NSCLC cells

Yu Zhang<sup>1\*</sup>, Ting-Qing Gan<sup>2\*</sup>, Xiao Wang<sup>3</sup>, Han-Lin Wang<sup>1</sup>, Xiu-Ling Zhang<sup>1</sup>, Yi-Wu Dang<sup>1</sup>, Su-Ning Huang<sup>4</sup>, Dian-Zhong Luo<sup>1</sup>, Ping Li<sup>1</sup>, Rong-Quan He<sup>2</sup>, Zu-Yun Li<sup>1</sup>, Gang Chen<sup>1</sup>

Departments of <sup>1</sup>Pathology, <sup>2</sup>Medical Oncology, <sup>4</sup>Radiotherapy, First Affiliated Hospital of Guangxi Medical University, Nanning, Guangxi Zhuang Autonomous Region, China; <sup>3</sup>Department of Orthopedics, China-Japan Union Hospital of Jilin University, Changchun, China. \*Equal contributors and co-first authors.

Received August 15, 2016; Accepted August 24, 2016; Epub March 1, 2017; Published March 15, 2017

**Abstract:** Background: Non-coding RNAs (ncRNAs), like long ncRNAs (lncRNAs) and microRNAs (miRNAs), are confirmed to play important roles in the tumorigenesis and deterioration of non-small cell lung cancer (NSCLC). However, the underlying expression profiling and prospective signal pathways of miRNAs associated with lncRNA HOXA11 antisense RNA (HOXA11-AS) in NSCLC remain unknown. Methods: HOXA11-AS was knocked down in A549 cell line and a microarray assay was used to detect the changes of the miRNA profiles. Four miRNA target prediction algorithms were applied to predict the potential target genes of the differentially expressed miRNAs. Bioinformatics analysis including Gene Ontology (GO), Kyoto Encyclopedia of Genes and Genomes (KEGG), protein-protein interactions (PPIs) and network analysis, were performed to investigate the potential functions, pathways and networks of the target genes. The different expression of HOXA11-AS between normal lung and NSCLC tissues was further verified by the data in The Cancer Genome Atlas (TCGA). Additionally, the relationship between the expression of HOXA11-AS and clinical diagnostic value was analyzed by receiver operating characteristic (ROC) curve. Results: Among all the miRNAs from the microarray, 43 and 18 miRNAs were upregulated and downregulated in NSCLC, respectively. According to the degree of the fold change, *p* value and false discovery rate (FDR), the top five upregulated and downregulated miRNAs were selected for further investigation. GO analysis on the target genes revealed that these de-regulated miRNAs were involved in complex cellular pathways, such as transcription, cell junction and transcription factor activity. KEGG pathway analysis showed that Wnt signaling pathway might be involved in regulating these 10 candidate miRNAs. XRN1 (degree = 23) and EP300 (degree = 20) had highest degree and interactions in the PPI network. Additionally, we found that HOXA11-AS was upregulated in lung adenocarcinoma and squamous cell carcinoma tissues based on TCGA database. The ROC curve revealed that the area under curve (AUC) of HOXA11-AS was 0.727 (95% CI 0.663~0.790) for lung adenocarcinoma and 0.933 (95% CI 0.906~0.960) for squamous cell carcinoma patients. Conclusions: Our results provide significant information on miRNAs related to HOXA11-AS in NSCLC and we hypothesize that HOXA11-AS might play a key role in NSCLC by regulating the expression of miRNAs through Wnt signaling pathway, which would be valuable for further investigation into the possible molecular mechanisms in NSCLC.

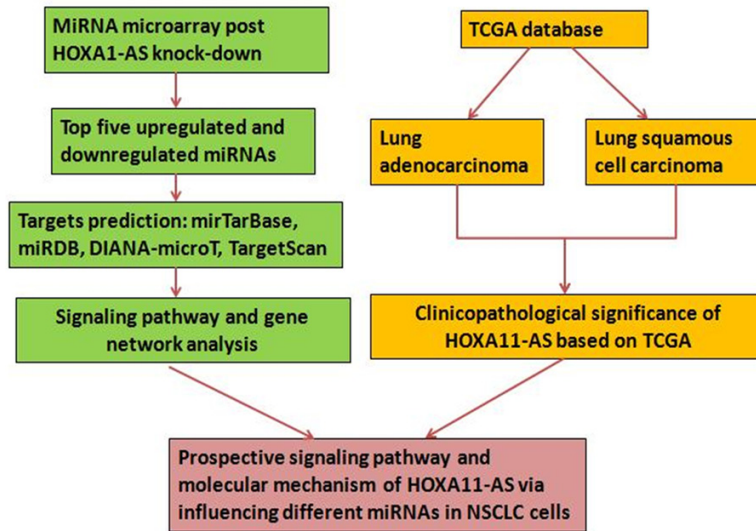
**Keywords:** HOXA11-AS, NSCLC, miRNA, GO, KEGG, pathway

## Introduction

Lung cancer has been one of the most commonly diagnosed cancers in the world, which is responsible for most of cancer death [1-4]. According to the histological type, lung cancer could be classified into two types: small cell lung cancer (SCLC) and non-small cell lung cancer (NSCLC). About 80%-85% of newly diag-

nosed lung cancers were NSCLC. NSCLC could be further divided into four subgroups: adenocarcinoma, squamous cell carcinoma, adenosquamous carcinoma and large cell carcinoma. More than 70% of new diagnostic NSCLC cases are advanced disease and the 5-year survival rate of patients diagnosed with NSCLC is only 16% [5]. Hence, further research into the possible molecular mechanisms in NSCLC tumori-

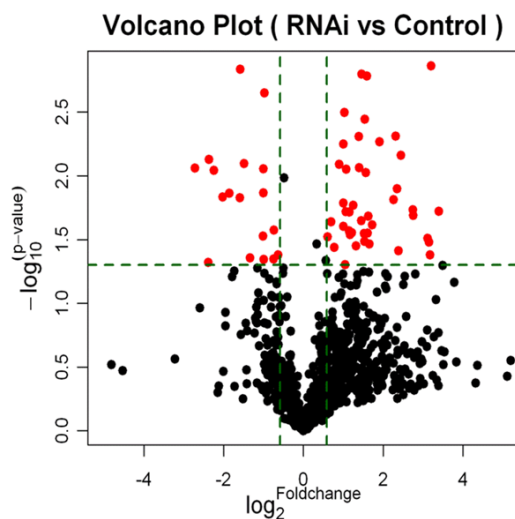
## Prospective target gene network of key miRNAs influenced by HOXA11-AS



**Figure 1.** A flow chart of this study.

**Table 1.** The sequences of HOXA11-AS siRNAs

ID	Target Seq	GC%
HOXA11-AS-RNAi(32154-2)	CTACCATCCCTGAGCCTTA	52.63%
HOXA11-AS-RNAi(32155-1)	TGACATCCGAGGAGACTTC	52.63%
HOXA11-AS-RNAi(32156-1)	CGTAATCGCCGGTGAAC	52.63%



**Figure 2.** Volcano plot for differentially expressed miRNAs after HOXA11-AS knock-down in NSCLC cells. Volcano plot was constructed through fold-change and *p* values, enabling visualization of the relationship between fold change (magnitude of change) and statistical significance.

genesis and deterioration is of great importance.

Long non-coding RNAs (lncRNAs) refer to RNAs without protein-coding capacity and the length of lncRNAs could vary from 200 nucleotides to 100 kilobases [6]. Many lncRNAs have been confirmed to play a part in transcriptional regulation, epigenetic gene regulation or disease development [7-10]. More importantly, lncRNAs can regulate the transcription of adjacent genes by combining the polymerases and transcription factors due to their wide distribution in nucleus [9, 11]. For example, lncRNAs could regulate the expression of miRNAs and their bio-function [6]. Therefore, the aberrant expression of lncRNAs could cause various human diseases and disorders [6].

MiRNAs are small noncoding RNAs with a length of 20 nucleotides. MiRNAs can play

important roles by regulating the expression of their target transcripts through interacting with the 3'-untranslated region (3'-UTR) [12-17]. The current researches have shown that miRNAs can play significant roles in NSCLC. Lan et al [18] found that miR-133a could be a tumor-suppressive miRNA in NSCLC, and the down-regulation of miR-133a suggested deterioration in NSCLC patients. Zhang et al [19] revealed that the downexpression of miRNA-320a could promote proliferation and invasion of NSCLC cells by increasing the expression of VDACL1. Zhu et al [20] found that miR-454 could promote the progression of NSCLC by directly targeting PTEN. The expression of miRNAs could also be regulated by lncRNA. Therefore, it is urgent to carry out a further exploration into miRNA profiling associated with lncRNA in NSCLC in order to seek novel therapeutic strategies.

In this study, we used microarray assay to detect the changes in the miRNA profiles of the A549 cells after HOXA11 antisense RNA (HOXA11-AS) knock-down. And four miRNA target prediction algorithms were applied to pre-

**Table 2.** The top 5 upregulated and top 5 downregulated miRNAs

ID	Name	Fold change	P value	Number of target genes
Upregulated miRNAs				
169152	miR-5690	9.178987	0.001371	835
46258	miR-1184	3.00934	0.001639	1192
148349	miR-3938	2.750255	0.001584	362
168985	miR-4722-5p	2.89295	0.003582	1696
169189	miR-4795-5p	4.946864	0.004853	604
Downregulated miRNAs				
46732	miR-1264	0.333113	0.00145	873
42673	miR-337-3p	0.50801	0.002232	458
11045	miR-302c-5p	0.498763	0.008787	2195
168642	miR-642b-3p	0.354892	0.007978	705
148317	miR-3621	0.497741	0.013555	40

dict the potential target genes of the differentially expressed miRNAs. Bioinformatics analysis including Gene Ontology (GO), Kyoto Encyclopedia of Genes and Genomes (KEGG), protein-protein interactions (PPIs) and network analysis, were performed to investigate the potential functions, pathways and networks of the target genes [21-24]. A flow chart of this study was shown in **Figure 1**.

## Materials and methods

### *Transfection with siRNA to knock-down HOXA11-AS in the NSCLC cell A549*

The human NSCLC A549 cell line obtained from the Type Culture Collection of the Chinese Academy of Sciences (Shanghai, China) was cultivated with 10% heat-inactivated fetal bovine serum (Invitrogen Corp, Grand Island, NY, USA) in a humidified atmosphere with 5% CO<sub>2</sub> at 37°C. Three HOXA11-AS specific siRNAs were synthesized by GenePharma (Shanghai, China) and merged into one siRNA pool (**Table 1**). The NSCLC A549 cell line was transfected with the HOXA11-AS siRNA for 72 hours. The Lipofectamine™2000 (Invitrogen, 11668-019) was utilized for the transfection on the manufacturer's instructions.

### *MiRNA microarray analysis*

The sample analysis and miRNA microarray hybridization were performed by Kangchen Biotech (Shanghai, China). Briefly, RNA Sample and RNA Sample QC were prepared. Buffer RPE was supplied as a concentrate. RNA was extracted and purified from 1 mg of total RNA

after removal of the rRNA (mRNA-ONLY Eukaryotic mRNA Isolation Kit, Epicentre Biotechnologies, Madison, USA). Then, each sample was transcribed and amplified into fluorescent cRNA by a random priming method. The cRNAs were labeled and hybridized through miRCURY™ Array Power Labeling kit (Cat #208032-A, Exiqon) and miRCURY™ Array, Wash buffer kit (Cat #208021, Exiqon), respectively. After the slides were washed, the arrays were scanned th-

rough the Axon GenePix 4000B microarray scanner. The GenePix pro V6.0 was used to read the raw intensity of the image. Median Normalization Method was applied for quantile normalization and subsequent data processing. Differentially expressed miRNAs between the groups of RNAi and the controls were identified as a fold change >1.5, P<0.05 as the cut-off.

### *MiRNA target prediction*

Four miRNA target prediction algorithms were applied to predict the potential target genes of the differentially expressed miRNAs. The four corresponding prediction algorithms were miRtarBase (available online: <http://mirtarbase.mbc.nctu.edu.tw/>), miRDB (available online: <http://www.mirdb.org/>), DIANA-microT (available online: <http://www.microrna.gr/microT>) and TargetScan (available online: <http://www.targetscan.org/>). And the comparison and identification of candidate genes were based on Venn diagrams (available online: <http://bioinformatics.psb.ugent.be/webtools/Venn/>).

### *GO and pathway analysis*

To better understand the underlying roles of the target genes, GO analysis and KEGG pathway analysis were applied based on biological process (BP), cellular component (CC) and molecular function (MF) as previously described [25]. The enrichment of the potential target genes was analyzed after being uploaded to the datasets of Database for Annotation, Visualization and Integrated Discovery (DAVID; available online: <http://david.abcc.ncifcrf.gov/>).

## Prospective target gene network of key miRNAs Influenced by HOXA11-AS

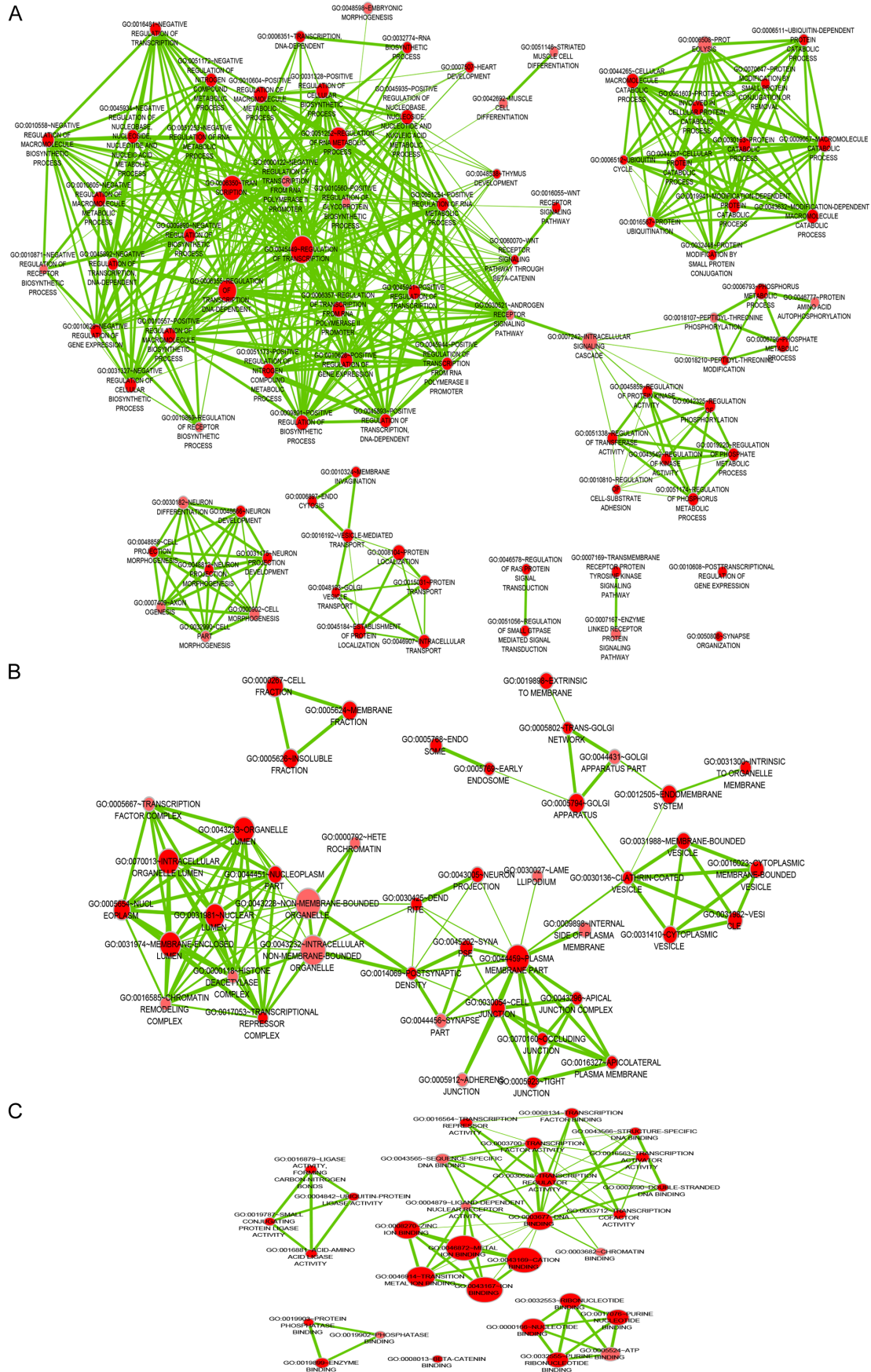
**Table 3.** GO functional annotation for most significantly related targets of miRNAs

GO ID	GO term	Fold Enrichment	P value	Gene symbol (top 30 genes)
<b>Biological process</b>				
GO:0006350	Transcription	1.44395	4.03E-12	NAA15, RORB, REST, RORA, CTNNB1, PRIM1, PGR, EPC1, TAF5L, ZNF776, ZNF772, ABRA, PATZ1, SAP30L, ZNF101, PHOX2B, ZNF641, ZNF100, C11ORF30, YY1, ZHX1, MECP2, MTPAP, ZNF649, ZHX3, MED14, ZNF793, MED13, PPARGC1A, MED10
GO:0045449	Regulation of transcription	1.348868	3.14E-10	HMG2, NAA15, RORB, RORA, REST, RAB1A, CTNNB1, PGR, EPC1, TAF5L, APP, ZNF776, ZNF772, ABRA, PATZ1, SAP30L, CCNA2, ZNF101, ZNF641, PHOX2B, ZNF100, RAN, C11ORF30, YY1, ZHX1, MECP2, ZNF649, ZHX3, MED14, MED13
GO:0045941	Positive regulation of transcription	1.79299	1.08E-08	NAA15, RORB, FOXO3, RORA, CTNNB1, WNT1, EPC1, APP, ABRA, CCNA2, CIITA, SATB2, MYO6, RAN, MED14, ARID1A, MED13, SIX4, MECOM, PPARGC1A, AHR, MAPK1, EP300, MTF1, HNF4A, TFAP2B, UBA52, ONECUT2, SOX6, MEIS2
GO:0010628	Positive regulation of gene expression	1.776048	1.25E-08	NAA15, RORB, FOXO3, RORA, CTNNB1, WNT1, EPC1, APP, ABRA, CCNA2, CIITA, SATB2, MYO6, RAN, MED14, ARID1A, MED13, SIX4, MECOM, PPARGC1A, AHR, MAPK1, EP300, MTF1, HNF4A, TFAP2B, UBA52, ONECUT2, SOX6, MEIS2
GO:0010557	Positive regulation of macromolecule biosynthetic process	1.719807	1.53E-08	NAA15, RORB, TLR4, RORA, FOXO3, CTNNB1, WNT1, EPC1, APP, ABRA, CCNA2, SAMD4A, SPN, CIITA, SATB2, IRS2, MYO6, RAN, MED14, ARID1A, MED13, SIX4, MECOM, PPARGC1A, AHR, MAPK1, EP300, MTF1, HNF4A, PDGFRA
<b>Cellular component</b>				
GO:0005794	Golgi apparatus	1.570991	3.79E-07	TGOLN2, VAPB, AP1G1, B3GALT4, PITPNB, IL17RD, RAB1A, TAPBP, HS2ST1, CUL3, APP, PICALM, UBXN2B, GNG2, PDGFD, SAR1B, MTUS1, RAB21, RAB27A, NMNAT2, PLD1, MYO6, STK25, BICD2, GLCE, GCC2, ERGIC2, GLUL, ATP2C1, VAMP7
GO:0030054	Cell junction	1.726642	1.66E-06	SYT1, LZTS1, GABRB3, GRIP1, GLRA3, GRIK3, STRN, ARHGAP17, ITSN1, ZNRF1, CXADR, AMOTL2, RHOU, CTNNB1, DNJC15, SNPH, GOPC, GRID2, SV2B, PARD3B, PAK1, SV2A, LRRC7, SAMD4A, ANKS1B, MAGI3, INADL, PSD3, VEZT, CTNNA1
GO:0044451	Nucleoplasm part	1.65233	6.74E-06	ARID4A, NR6A1, NAA15, INTS2, ZNF638, ZEB1, RLIM, GLI3, CBX5, CTNNB1, EPC1, TAF5L, CSNK2A1, GTF2A1, OIP5, LUC7L3, TBL1XR1, ANKS1B, SATB2, MYO6, YY1, TP53, CDK8, GTF2H3, MED14, RB1, MED13, PPP1CC, PPP1CB, PPARGC1A
GO:0019898	Extrinsic to membrane	1.350775	1.88E-05	TGOLN2, RNMT, NAA15, SNRPD1, SYNCRIP, INTS2, ZNF638, CBX5, CTNNB1, KLHL7, PRIM1, EPC1, TAF5L, CSNK2A1, OIP5, TARDBP, SAP30L, CCNA2, LUC7L3, LRRC7, OXR1, PABPN1, GTPBP4, SATB2, MYO6, DFFA, RAN, YY1, GABPA, HNRNPA2B1
GO:0005654	Nucleoplasm	1.463326	2.63E-05	RNMT, NAA15, SNRPD1, SYNCRIP, INTS2, ZNF638, CBX5, CTNNB1, PRIM1, EPC1, TAF5L, CSNK2A1, OIP5, CCNA2, LUC7L3, PABPN1, SATB2, MYO6, DFFA, RAN, YY1, HNRNPA2B1, MED14, MED13, PPP1CC, PPP1CB, PPARGC1A, MED10, ELL2, SUZ12
<b>Molecular function</b>				
GO:0008270	Zinc ion binding	1.327066	2.69E-08	GDA, DZIP1, RNF217, RORB, ZNF638, REST, MYLIP, RORA, ZNRF1, RNF212, ZNRF3, PRIM1, PGR, APP, ZNF776, ZNF772, PATZ1, ZNF101, ZNF641, ZNF100, YY1, ZHX1, ZNF649, ZHX3, ZNF793, MECOM, RNF222, ZNF37A, ADAMTS9, NAPEPLD
GO:0046914	Transition metal ion binding	1.273725	1.39E-07	GDA, PDP2, DZIP1, RNF217, RORB, ZNF638, RORA, REST, MYLIP, ZNRF1, RNF212, ZNRF3, PRIM1, PGR, APP, ZNF776, ZNF772, PATZ1, ZNF101, ZNF641, ZNF100, YY1, ZHX1, ZNF649, ZHX3, NUDT11, ZNF793, MECOM, RNF222, ZNF37A
GO:0003677	DNA binding	1.302523	2.21E-07	XRCC2, HMG2, LEMD3, RORB, ZNF638, REST, RORA, CTNNB1, PGR, TAF5L, APP, ZNF776, ZNF772, PATZ1, LUC7L3, ZNF101, PHOX2B, ZNF641, ZNF100, YY1, ZHX1, MECP2, ZHX3, ZNF649, ZNF793, H2AFJ, MECOM, PPARGC1A, ZNF37A, HNF4A
GO:0030528	Transcription regulator activity	1.37251	1.00E-06	RORB, REST, RORA, CTNNB1, PGR, EPC1, TAF5L, ABRA, PATZ1, PHOX2B, RAN, YY1, ZHX1, MECP2, ZHX3, MED14, MED13, MECOM, PPARGC1A, MED10, ZNF37A, HNF4A, MTF1, MLLT10, FOXG1, SHOX, VGLL3, ELL, TFAP2L1, ZNF131
GO:0003700	Transcription factor activity	1.425954	1.37E-05	RORB, RORA, FOXO3, CTNNB1, PGR, TAF5L, TARDBP, ZNF445, PHOX2B, SATB1, SATB2, YY1, GABPA, ZHX1, ZHX3, FOXN2, SIX4, MECOM, AHR, FOXN3, ZNF37A, EP300, MTF1, HNF4A, ZNF197, MLLT10, FOXG1, TFAP2B, MGA, TFAP2A

Note: GO, Gene Ontology.



# Prospective target gene network of key miRNAs influenced by HOXA11-AS



## Prospective target gene network of key miRNAs Influenced by HOXA11-AS

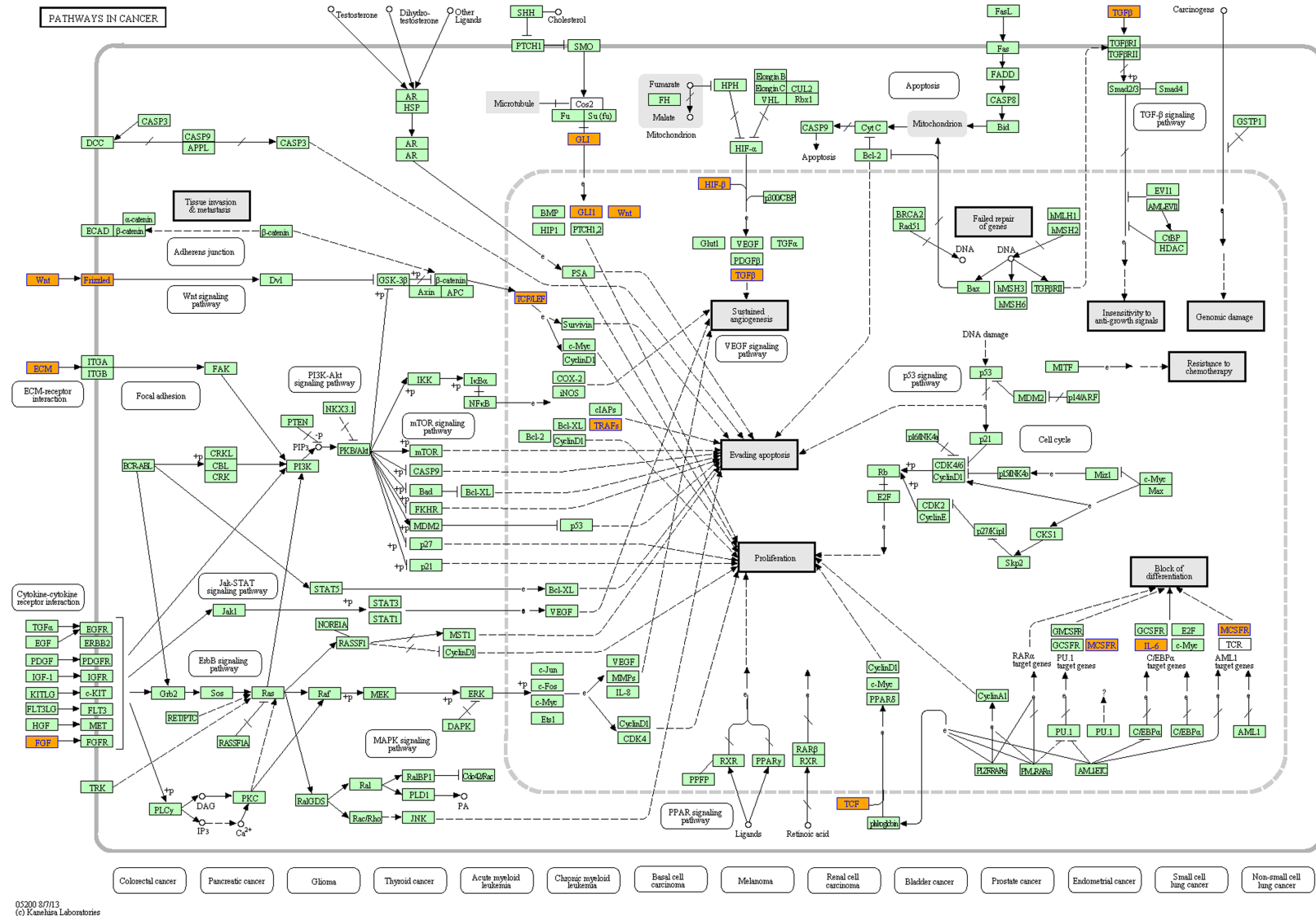
**Figure 3.** A function network of Gene Ontology (GO) terms for the target genes of 10 miRNAs in NSCLC. A. Biological process (BP). B. Cellular component (CC). C. Molecular function (MF).

**Table 4.** KEGG pathway enrichment analysis of miRNAs

KEGG ID	KEGG term	Fold Enrichment	P value	Gene symbol
hsa04310	Wnt signaling pathway	2.711163	1.70E-08	APC2, CAMK2G, PPP2R5C, DAAM1, TCF7L2, PRKX, TCF7L1, CTNNB1, WNT1, PLCB3, CSNK2A1, WNT3, CACYBP, CAMK2D, FRAT1, NFATC4, NFATC2, FBXW11, NFATC3, CSNK1A1, TBL1XR1, VANGL1, LY6G5B, NLK, CREBBP, TP53, FZD3, FZD4, FZD7, DKK2, EP300, CCND2, GSK3B, LRP6, PPP2R5E, TBL1X
hsa05213	Endometrial cancer	3.729221	2.09E-06	APC2, PIK3CB, TP53, MLH1, FOXO3, CTNNA1, TCF7L2, TCF7L1, CTNNB1, MAPK1, NRAS, PDPK1, KRAS, CASP9, GSK3B, SOS1, PIK3R1
hsa05215	Prostate cancer	2.905161	3.54E-06	AR, PIK3CB, CREB1, CREBBP, TP53, CREB5, RB1, TCF7L2, TCF7L1, CTNNB1, MAPK1, NRAS, PDPK1, KRAS, EP300, CASP9, GSK3B, SOS1, PDGFRA, MDM2, TGFA, PDGFD, PIK3R1
hsa05200	Pathways in cancer	1.773654	2.72E-05	MITF, MLH1, FGF13, GLI3, PTEN, CTNNB1, WNT1, WNT3, CASP9, TGFA, AR, PLD1, PIK3CB, RUNX1T1, TP53, RB1, CTNNA1, MECOM, FGF20, RAD51, MAPK1, CCDC6, CRKL, EP300, NCOA4, PDGFRA, MDM2, MAPK8, TRAF1, APC2, EGLN3, TCF7L2, TCF7L1, TPM3, KRAS, ITGAV, SOS1, PIK3R1, COL4A4, BMP2, COL4A1, TGFBR1, MET, CREBBP, CBL, FZD3, APPL1, FZD4, FZD7, NRAS, HDAC2, PLCG1, GSK3B, JAK1

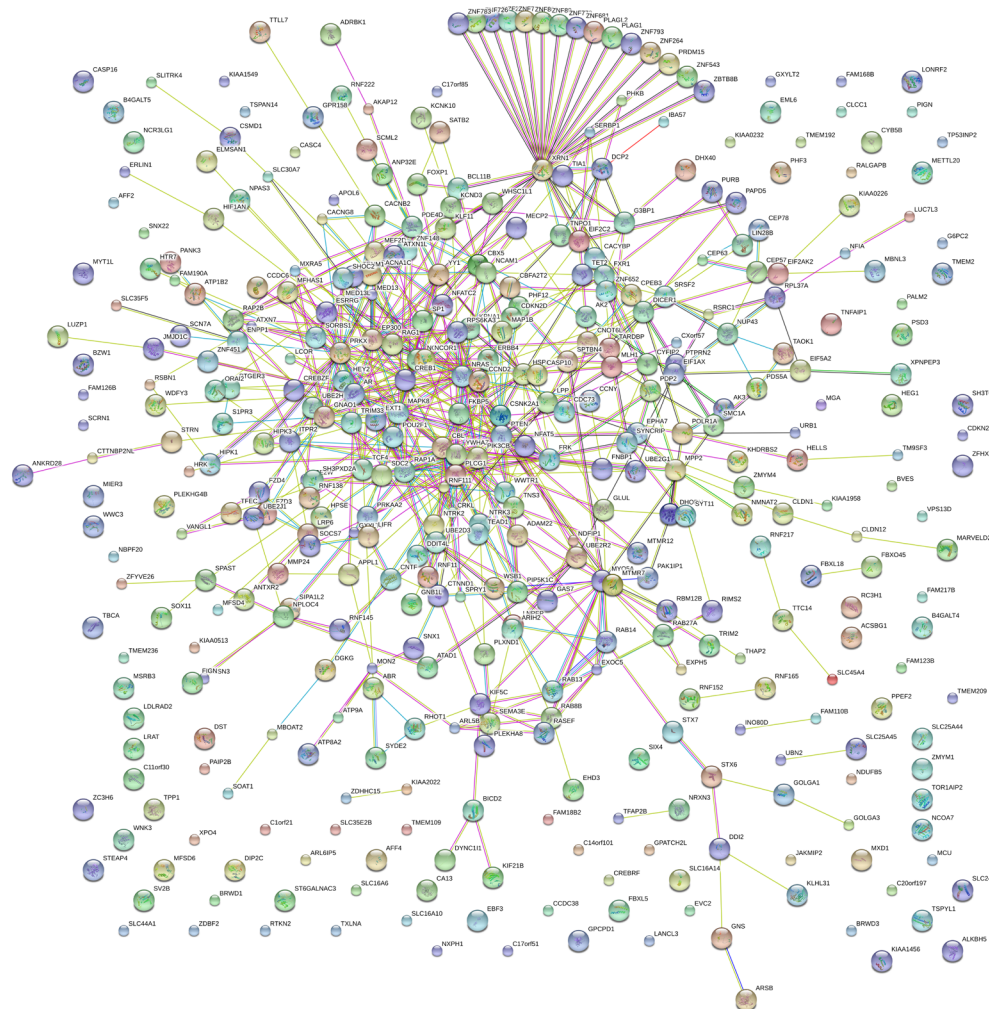
Notes: KEGG, Kyoto Encyclopedia of Genes and Genomes.

## Prospective target gene network of key miRNAs Influenced by HOXA11-AS



**Figure 4.** Important signal pathway by bioinformatics analysis. KEGG pathway analysis showed that Wnt signaling pathway and pathways in cancer were responsible for the bio-function of the 10 candidate miRNAs.



## Prospective target gene network of key miRNAs influenced by HOXA11-AS





### Nodes:

Network nodes represent proteins  
splice isoforms or post-translational modifications are collapsed, i.e. each node represents all the proteins produced by a single, protein-coding gene locus.

### Node Size

-  small nodes:  
protein of unknown 3D structure
-  large nodes:  
some 3D structure is known or predicted

### Node Color

-  colored nodes:  
query proteins and first shell of interactors
-  white nodes:  
second shell of interactors

### Edges:

Edges represent protein-protein associations

associations are meant to be specific and meaningful, i.e. proteins jointly contribute to a shared function; this does not necessarily mean they are physically binding each other.

### Edge Confidence

-  low (0.150)
-  medium (0.400)
-  high (0.700)
-  highest (0.900)

**Figure 5.** The PPI network of DEGs.

Genes with false discovery rate (FDR)  $\leq 0.05$  and  $P < 0.05$  were identified to be obviously enriched in the target genes.

### Construction of protein-protein interaction (PPI) network

The interaction pairs of target genes were investigated through Search Tool for the Retrieval of Interacting Genes (STRING; version 9.0,

<http://string-db.org>) [26]. STRING was a database of known and predicted PPIs. A combined score  $> 0.4$  was selected to construct the PPI network.

### Additional analysis of the differentially expressed miRNAs in NSCLC from TCGA

TCGA (<http://cancergenome.nih.gov/>) is an overall collection of SNP array, exome sequenc-



ing, miRNA-seq, RNA-seq and data DNA methylation, and so on [27]. TCGA could also be applied to analyze complicated cancer genomics and clinical parameters [28, 29]. In this study, the original data of RNASeqV2 in lung adenocarcinoma and squamous cell carcinoma were extracted from TCGA. Then the expression level of HOXA11-AS in each case was calculated according to the distribution of exon reads. Also, we extracted the co-genes of HOXA11-AS in TCGA through R Project for Statistical Computing (<https://www.r-project.org/>). A FDR <0.05 was considered for co-expressed relationship.

## Statistical analysis

SPSS 20.0 was used for the statistical analysis. The t-test was applied for comparing the expression of HOXA11-AS in lung adenocarcinoma and squamous cell carcinoma. And the relationship between the expression of HOXA11-AS and clinical diagnostic value was analyzed by ROC curve. P<0.05 was considered statistically significant (two-sides).

## Results

### *MiRNAs profiling associated with lncRNA HOXA11-AS*

The transfection efficiency was approximately 100%, and the knock-down efficiency of HOXA11-AS in NSCLC cell lines were over 75% as detected by real time RT-qPCR (data not shown). Then a miRNA microarray assay was performed to detect differential expression profiles of miRNAs between the groups of HOXA11-AS RNAi and control in A549 cell lines in triplicate. Forty-three upregulated and 18 downregulated miRNAs were found differentially expressed. A summary of these differentially expressed miRNAs was presented in the volcano plot (**Figure 2**). The fold changes (HOXA11-AS-RNAi vs. HOXA11-AS-control) and P values were calculated after the expression values were standardized. The top 10 miRNAs were selected as most significant differentially expressed miRNAs (fold change  $\geq 1.5$  or  $< 1$  and  $P < 0.05$ ), among which, five miRNAs were upregulated and five miRNAs were downregulated (**Table 2**).

### *MiRNA target prediction*

In this study, four miRNA target prediction algorithms (miRtarBase, miRDB, DIANA-microT and

TargetScan) were applied to predict the potential target genes of the differentially expressed miRNAs. And Venn diagrams were used to compare and identify the candidate genes. The genes predicted by more than two algorithms were selected as the final target candidate genes. And the number of these target candidate genes of each miRNA was shown in **Table 2**.

### *GO and pathway analysis*

Among all these target genes, 1914 genes were selected for prediction by more than two miRNAs, and these genes were used to perform GO and pathway analysis (**Supplementary Table 1**). The GO analysis identified BP, CC and MF which the target genes may be involved in. The GO functional annotation for most significantly related targets of miRNAs were shown in **Table 3**. And GO analysis showed the most significant functional groups, such as transcription, cell junction and transcription factor activity. To better reveal the relevant functions of the target genes, a function network of BP, CC and MF was constructed based on the GO analysis with Cytoscape (**Figure 3**).

The KEGG analysis showed that the target genes might be involved in different pathways. A total of four relevant pathways were available through the pathway analysis ( $FDR \leq 0.05$ ,  $P < 0.05$ , **Table 4**). The two mostly relevant pathways (Wnt signaling pathway, Pathways in cancer) were involved in NSCLC development and progression as previously reported. As was shown in Pathways in cancer (**Figure 4**),  $\beta$ -catenin activity played an important role in Wnt signaling pathway. An inappropriate activation of the Wnt/ $\beta$ -catenin signaling pathway might lead to the development of human cancers, such as lung cancer.

### *PPI network analysis*

The PPI network was constructed by STRING and a total of 621 PPI pairs with combined score  $> 0.4$  were selected. The map of PPI network was available in **Figure 5**. And the number of nodes was 405, accounting for 21.16% of all target genes. The PPI network had high cluster properties, and the clustering coefficient was 0.613. XRN1 (degree = 23) and EP300 (degree = 20) had high degrees and interactions in the PPI network. Then a sub-network of 173 PPI




[illegible]


**Nodes:**

**Network nodes represent proteins**


*splice isoforms or post-translational modifications are collapsed, i.e. each node represents all the proteins produced by a single, protein-coding gene locus.*


**Node Size**

 *small nodes: protein of unknown 3D structure*

 *large nodes: some 3D structure is known or predicted*

**Node Color**

 *colored nodes: query proteins and first shell of interactors*

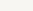
 *white nodes: second shell of interactors*


**Edges:**


**Edges represent protein-protein associations**


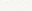
*associations are meant to be specific and meaningful, i.e. proteins jointly contribute to a shared function; this does not necessarily mean they are physically binding each other.*

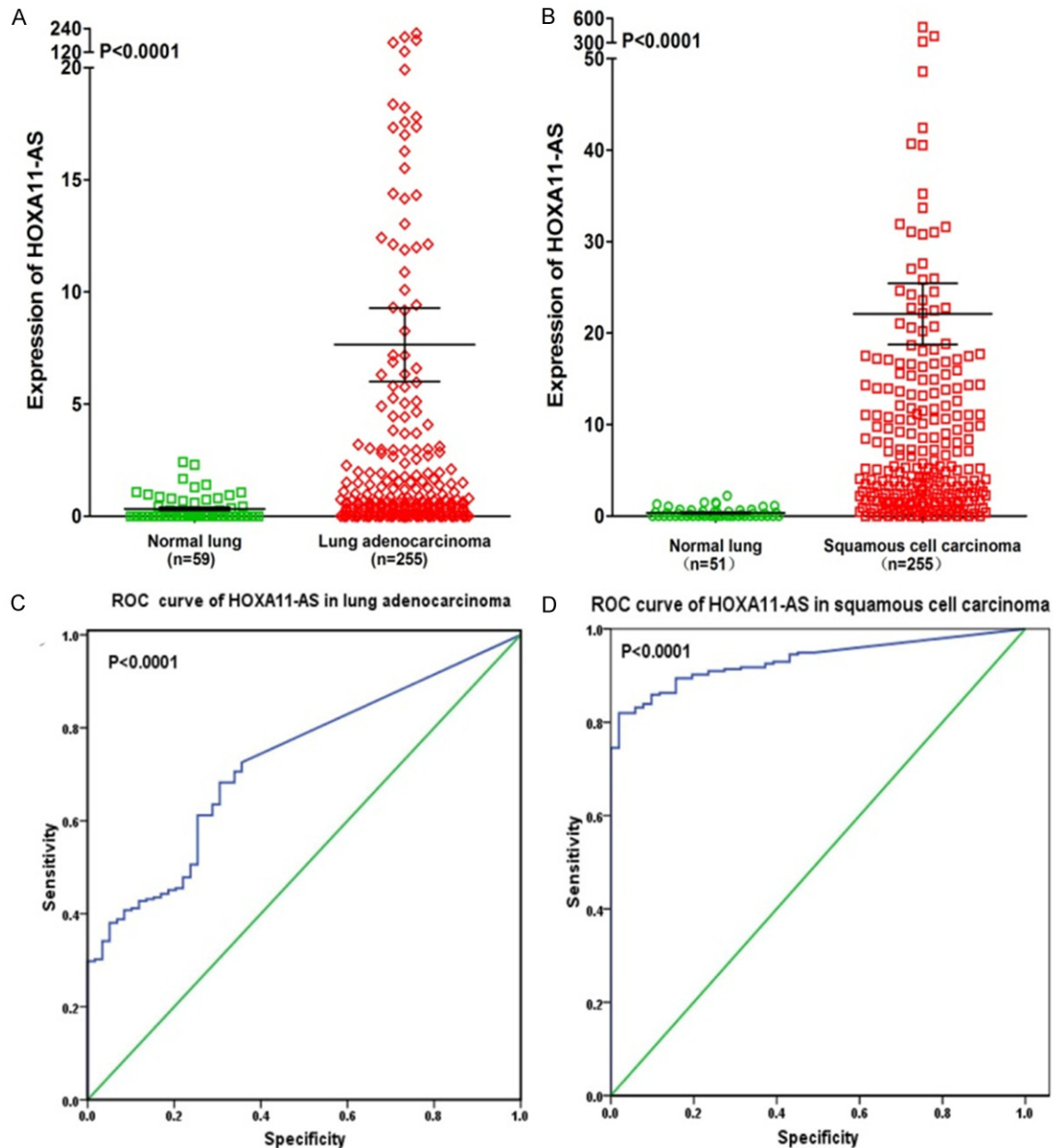
**Edge Confidence**

  *low (0.150)*

  *medium (0.400)*

  *high (0.700)*

  *highest (0.900)*



**Figure 7.** Differential expression and ROC curve of HOXA11-AS in lung adenocarcinoma and squamous cell carcinoma based on The Cancer Genome Atlas (TCGA) database. A. Differential expression of HOXA11-AS in lung adenocarcinoma. B. Differential expression of HOXA11-AS in squamous cell carcinoma. C. ROC curve of HOXA11-AS in lung adenocarcinoma. D. ROC curve of HOXA11-AS in squamous cell carcinoma.

pairs was selected for further analyses, whose connectivity degrees were more than 10 as presented in **Figure 6**.

#### Supplementary information from the Cancer Genome Atlas (TCGA) database

In order to reveal the relationship between HOXA11-AS and NSCLC, we performed a clini-

cal study with the original data in TCGA. We found that HOXA11-AS was upregulated in both lung adenocarcinoma ( $7.645 \pm 1.641$  vs.  $0.330 \pm 0.075$ ) and squamous cell carcinoma ( $22.090 \pm 3.348$  vs.  $0.353 \pm 0.072$ ) compared to non-cancerous lung tissues (both  $P < 0.0001$ , **Figure 7A, 7B**). And the ROC curve revealed that the area under curve (AUC) of HOXA11-AS was 0.727 (95% CI 0.663~0.790) for lung ad-





**Figure 8.** HOXA11-AS-co-genes network in lung adenocarcinoma by bioinformatics analysis. Three hundred and ninety-seven co-genes were extracted in lung adenocarcinoma. And the relationships between HOXA11-AS and these co-genes were easily observed from this network analysis.

enocarcinoma patients and 0.933 (95% CI 0.906~0.960) for squamous cell carcinoma patients (both  $P < 0.0001$ ), which could gain high diagnostic value of HOXA11-AS level in lung cancer (**Figure 7C, 7D**).

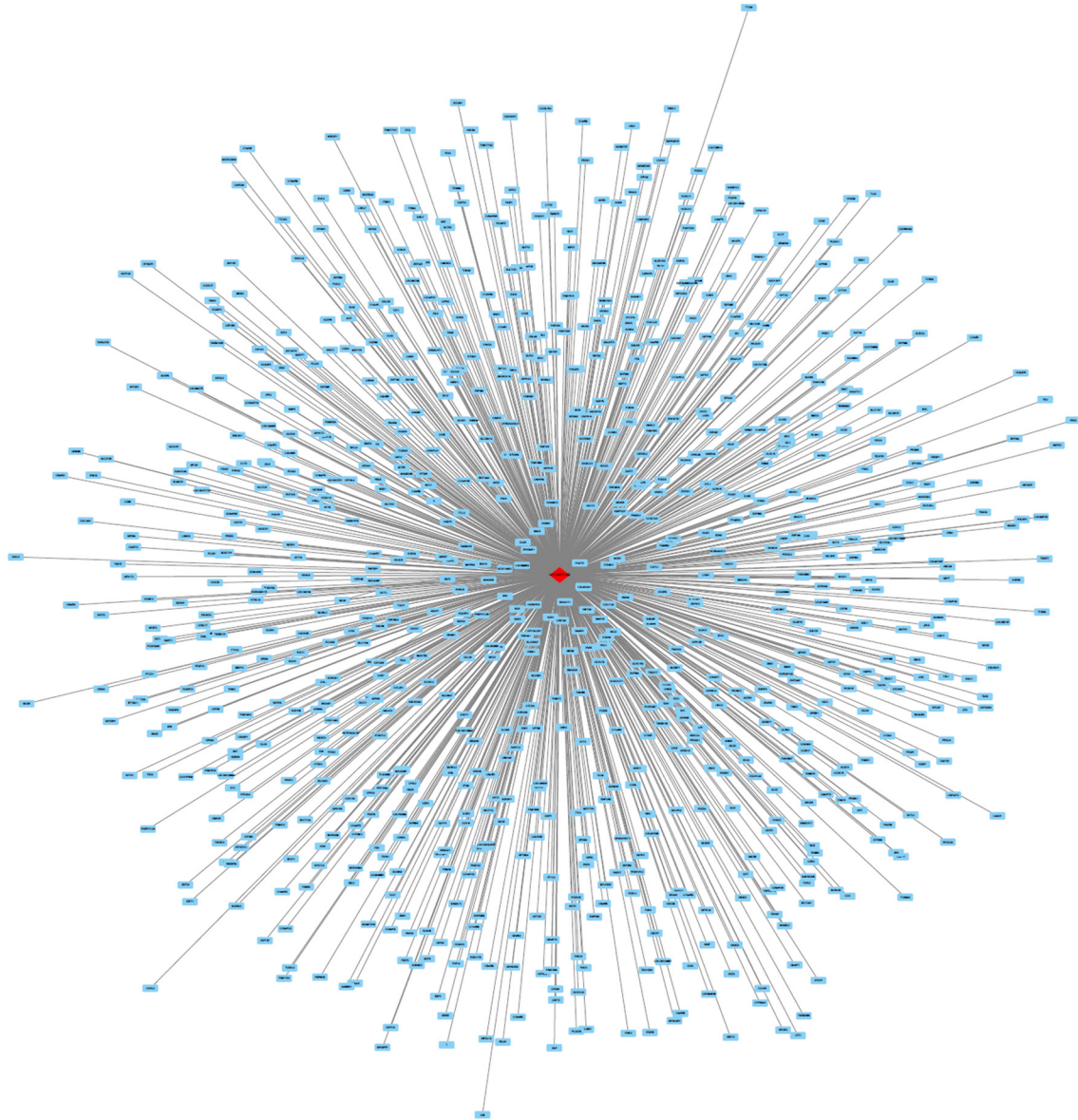
Also, the co-genes of HOXA11-AS in TCGA were extracted through R Project for Statistical Computing. And 397 co-genes were extracted in lung adenocarcinoma and 899 co-genes were extracted in squamous cell carcinoma. Additionally, gene networks of HOXA11-AS and its co-genes, miRNAs and their target genes were constructed in the present study (**Figures 8-10**). And the relationships between HOXA11-AS and its co-genes, miRNAs and their target genes were easily observed from this network analysis.

## Discussion

LncRNAs constitute the majority of the non-coding RNAs. And lncRNAs are novel key elements in regulating different cellular processes, such as transcription, activity of protein [30]. Also, lncRNAs have been reported to be associated with tumorigenesis and progression of NSCLCs. To date, several lncRNAs have been reported to play a vital part in NSCLC, such as lncRNA TATDN1, RGMB-AS1 and MALAT1, which may relate to cell proliferation, invasion and metastasis of NSCLC [31-33]. And growing evidence has shown that lncRNAs may play significant roles by regulating miRNAs expression in lung cancer. For example, lncRNA CCAT1 could downregulate miR-218 levels via BMI1 to promote cell cycle transition in cigarette smoke extract-induced lung carcinogenesis [34]. lncRNA UCA1 could perform oncogenic functions in NSCLC by targeting miR-193a-3p [35]. HOXA11-AS is a member of the homeobox (HOX) family of genes. Until now, only two studies have reported the relationship between HOXA11-AS and cancer. Richards et al [36] conducted various functional experiments and analyzed genome-wide data and then found that HOXA11-AS could inhibit the oncogenic phenotype of epithelial ovarian cancer. Wang et al [37] used a high-throughput microarray and gene set enrichment analysis to demonstrate that HOXA11-AS was a cell cycle-associated

lncRNA and might be a biomarker for identifying glioma progression. However, the particular pathogenesis of HOXA11-AS in NSCLC is still vague. Previously, we detected the expression of HOXA11-AS in four NSCLC cell lines (A549, H460, 1299 and PC9) and A549 cell lines gained the highest HOXA11-AS expression level (data not shown). Thus, we designed this study on A549 cells to explore miRNAs expression profile changes after HOXA11-AS knock-down, and clarify the possible molecular mechanisms of HOXA11-AS in NSCLC.

In this study, a microarray assay was used to detect changes in the miRNA profiles of A549 cells. Among all the differentially expressed miRNAs, the top five upregulated (miR-5690, miR-1184, miR-3938, miR-4722-5p, miR-4795-5p) and downregulated miRNAs (miR-1264, miR-337-3p, miR-302c-5p, miR-642b-3p, and miR-3621) were selected for further investigation. GO analysis of the target genes revealed that these de-regulated miRNAs were mainly related to transcription, cell junction and transcription factor activity. After analyzing the original data from TCGA database, we found that HOXA11-AS was upregulated in both lung adenocarcinoma and squamous cell carcinoma. Also, the ROC curve revealed that the HOXA11-AS level might have important value in diagnosis of lung cancer. Then the possible pathways of HOXA11-AS in lung cancer were investigated. According to the results of KEGG pathway analysis, Wnt signaling pathway might be involved in regulating these 10 candidate miRNAs. Up to now, many reports have demonstrated that Wnt signaling pathway was related to NSCLC cell growth, invasion and metastasis [38-40]. Jiang et al [38] found that the overexpression of miR-376c could suppresses cell growth and invasion of NSCLC by regulating LHR-1-mediated Wnt signaling pathway. Su et al [39] demonstrated that CD44 could promote metastatic activity in CD133+ CD44+ lung cancer stem cell-like cells through Wnt/ $\beta$ -catenin pathway. Tong et al [40] found that ART, DHA, and ARTS could inhibit lung-tumor progression by suppressing Wnt/ $\beta$ -catenin pathway. However, the effect and mechanism of HOXA11-AS remains unclear in NSCLC. According to the aforementioned results, we hypothesized that miRNAs



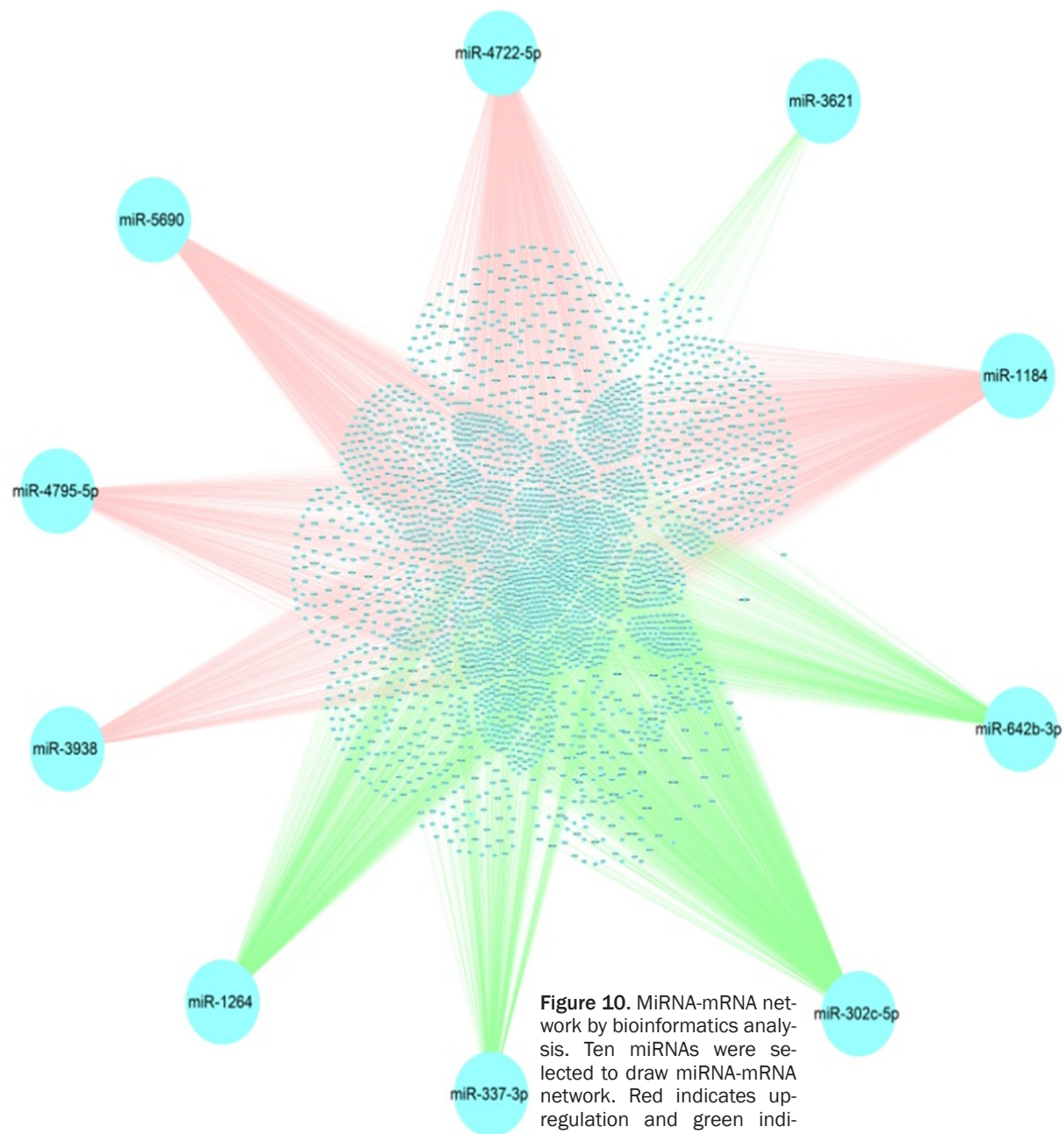
**Figure 9.** HOXA11-AS-co-genes network in squamous cell carcinoma by bioinformatics analysis. Eight hundred and ninety-nine co-genes were extracted in lung adenocarcinoma. And the relationships between HOXA11-AS and these co-genes were easily observed from this network analysis.

regulated by lncRNA HOXA11-AS might play important roles in NSCLC tumorigenesis and deterioration via Wnt signaling pathway. But further exploration is still needed to clarify the possible molecular mechanisms of HOXA11-AS in NSCLC tumorigenesis and deterioration. To verify this hypothesis, we plan to perform a series of experiments, including real time RT-qPCR, in situ hybridization, dual luciferase reporter assay, RNA binding protein immunoprecipitation (RIP), RNA pull-down, chromatin

immunoprecipitation (ChIP), western blot, invasion and metastasis assays, chicken embryo-chorioallantoic membrane and nude mouse models. The clinical significance, the effect and molecular mechanism of HOXA11-AS on the biological function of NSCLC cells will be investigated from perspectives of molecule, cell, tissue and animal. Focusing on the new insight of HOXA11-AS/miRNAs/genes axis, this study aims to provide a novel target for clinical prevention and therapeutic strategy of NSCLC.



# Prospective target gene network of key miRNAs Influenced by HOXA11-AS



**Figure 10.** MiRNA-mRNA network by bioinformatics analysis. Ten miRNAs were selected to draw miRNA-mRNA network. Red indicates up-regulation and green indicates downregulation.

## Conclusion

In summary, HOXA11-AS might play an important role via influencing several key miRNAs in different biological processes of NSCLC by targeting their specific target genes. Original data from TCGA further verified the oncogenic role of HOXA11-AS in both lung adenocarcinoma and squamous cell carcinoma. These results could be valuable for further researches on the relationship between HOXA11-AS and the possible molecular mechanisms in NSCLC tumorigenesis and deterioration.

## Acknowledgements

The study was supported by Fund of the Guangxi Provincial Health Bureau Scientific Research Project (Z2013201, Z2014055), Fund of the National Natural Science Foundation of China (NSFC81360327, NSFC815-60469), the Natural Science Foundation of Guangxi, China (2015GXNSFCA139009) and the Scientific Research Project of the Basic Ability Promoting for Middle Age and Youth Teachers of Guangxi Universities (KY2016YB-077). The funders had no role in the study design, the data collection and analysis, the decision to publish, or the preparation of the manuscript. Yu Zhang and Ting-Qing Gan contributed equally as co-first authors, and Zu-Yun Li and Gang Chen contributed equally as co-corresponding authors of this paper.

## Disclosure of conflict of interest

None.

**Address correspondence to:** Drs. Zu-Yun Li and Gang Chen, Department of Pathology, First Affiliated Hospital of Guangxi Medical University, 6 Shuang-yong Road, Nanning 530021, Guangxi Zhuang Autonomous Region, China. E-mail: lizuyun8877@aliyun.com (ZYL); chen\_gang\_triones@163.com (GC)

## References

- [1] Xu YJ, Du Y and Fan Y. Long noncoding RNAs in lung cancer: what we know in 2015. *Clin Transl Oncol* 2016; 18: 660-665.
- [2] Kang CG, Lee HJ, Kim SH and Lee EO. Zerumbone Suppresses Osteopontin-Induced Cell Invasion Through Inhibiting the FAK/AKT/ROCK Pathway in Human Non-Small Cell Lung Cancer A549 Cells. *J Nat Prod* 2016; 79: 156-160.
- [3] Xu G, Chen J, Pan Q, Huang K, Pan J, Zhang W, Chen J, Yu F, Zhou T and Wang Y. Long noncoding RNA expression profiles of lung adenocarcinoma ascertained by microarray analysis. *PLoS One* 2014; 9: e104044.
- [4] Choe C, Shin YS, Kim C, Choi SJ, Lee J, Kim SY, Cho YB and Kim J. Crosstalk with cancer-associated fibroblasts induces resistance of non-small cell lung cancer cells to epidermal growth factor receptor tyrosine kinase inhibition. *Onco Targets Ther* 2015; 8: 3665-3678.
- [5] Chen G, Umelo IA, Lv S, Teugels E, Fostier K, Kronenberger P, Dewaele A, Sadones J, Geers C and De Greve J. miR-146a inhibits cell growth, cell migration and induces apoptosis in non-small cell lung cancer cells. *PLoS One* 2013; 8: e60317.
- [6] Xie X, Pan J, Wei L, Wu S, Hou H, Li X and Chen W. Gene expression profiling of microRNAs associated with UCA1 in bladder cancer cells. *Int J Oncol* 2016; 48: 1617-1627.
- [7] Wilusz JE. Long noncoding RNAs: Re-writing dogmas of RNA processing and stability. *Biochim Biophys Acta* 2016; 1859: 128-138.
- [8] Yuan X, Wang J, Tang X, Li Y, Xia P and Gao X. Berberine ameliorates nonalcoholic fatty liver disease by a global modulation of hepatic mRNA and lncRNA expression profiles. *J Transl Med* 2015; 13: 24.
- [9] Ponting CP, Oliver PL and Reik W. Evolution and functions of long noncoding RNAs. *Cell* 2009; 136: 629-641.
- [10] Wei Y and Niu B. Role of MALAT1 as a Prognostic Factor for Survival in Various Cancers: A Systematic Review of the Literature with Meta-Analysis. *Dis Markers* 2015; 2015: 164635.
- [11] Wang X, Song X, Glass CK and Rosenfeld MG. The long arm of long noncoding RNAs: roles as sensors regulating gene transcriptional programs. *Cold Spring Harb Perspect Biol* 2011; 3: a003756.
- [12] Bartel DP. MicroRNAs: genomics, biogenesis, mechanism, and function. *Cell* 2004; 116: 281-297.
- [13] He L and Hannon GJ. MicroRNAs: small RNAs with a big role in gene regulation. *Nat Rev Genet* 2004; 5: 522-531.
- [14] Tay Y, Zhang J, Thomson AM, Lim B and Rigoutsos I. MicroRNAs to Nanog, Oct4 and Sox2 coding regions modulate embryonic stem cell differentiation. *Nature* 2008; 455: 1124-1128.
- [15] Yang H, Tang Y, Guo W, Du Y, Wang Y, Li P, Zang W, Yin X, Wang H, Chu H, Zhang G and Zhao G. Up-regulation of microRNA-138 induce radiosensitization in lung cancer cells. *Tumour Biol* 2014; 35: 6557-6565.
- [16] Tang R, Liang L, Luo D, Feng Z, Huang Q, He R, Gan T, Yang L and Chen G. Downregulation of MiR-30a is Associated with Poor Prognosis in Lung Cancer. *Med Sci Monit* 2015; 21: 2514-2520.

- [17] Wu S, Shen W, Pan Y, Zhu M, Xie K, Geng L, Wang Y, Liang Y, Xu J, Cao S, Xu W, Chen B, Hu Z, Ma H, Wu J and Shen H. Genetic Variations in Key MicroRNAs are Associated With the Survival of Non-small Cell Lung Cancer. *Medicine (Baltimore)* 2015; 94: e2084.
- [18] Lan D, Zhang X, He R, Tang R, Li P, He Q and Chen G. MiR-133a is downregulated in non-small cell lung cancer: a study of clinical significance. *Eur J Med Res* 2015; 20: 50.
- [19] Zhang G, Jiang G, Wang C, Zhong K, Zhang J, Xue Q, Li X, Jin H and Li B. Decreased expression of microRNA-320a promotes proliferation and invasion of non-small cell lung cancer cells by increasing VDAC1 expression. *Oncotarget* 2016; [Epub ahead of print].
- [20] Zhu DY, Li XN, Qi Y, Liu DL, Yang Y, Zhao J, Zhang CY, Wu K and Zhao S. MiR-454 promotes the progression of human non-small cell lung cancer and directly targets PTEN. *Biomed Pharmacother* 2016; 81: 79-85.
- [21] Xu X, Wang X, Fu B, Meng L and Lang B. Differentially expressed genes and microRNAs in bladder carcinoma cell line 5637 and T24 detected by RNA sequencing. *Int J Clin Exp Pathol* 2015; 8: 12678-12687.
- [22] Li Q, Ge X, Xu X, Zhong Y and Qie Z. Comparison of the gene expression profiles between gallstones and gallbladder polyps. *Int J Clin Exp Pathol* 2014; 7: 8016-8023.
- [23] Jiang CM, Wang XH, Shu J, Yang WX, Fu P, Zhuang LL and Zhou GP. Analysis of differentially expressed genes based on microarray data of glioma. *Int J Clin Exp Med* 2015; 8: 17321-17332.
- [24] Chen L, Zhuo D, Chen J and Yuan H. Screening feature genes of lung carcinoma with DNA microarray analysis. *Int J Clin Exp Med* 2015; 8: 12161-12171.
- [25] Ashburner M, Ball CA, Blake JA, Botstein D, Butler H, Cherry JM, Davis AP, Dolinski K, Dwight SS, Eppig JT, Harris MA, Hill DP, Issel-Tarver L, Kasarskis A, Lewis S, Matese JC, Richardson JE, Ringwald M, Rubin GM and Sherlock G. Gene ontology: tool for the unification of biology. The Gene Ontology Consortium. *Nat Genet* 2000; 25: 25-29.
- [26] Franceschini A, Szklarczyk D, Frankild S, Kuhn M, Simonovic M, Roth A, Lin J, Minguez P, Bork P, von Mering C and Jensen LJ. STRING v9.1: protein-protein interaction networks, with increased coverage and integration. *Nucleic Acids Res* 2013; 41: D808-815.
- [27] Bornstein S, Schmidt M, Choonoo G, Levin T, Gray J, Thomas CR Jr, Wong M and McWeeney S. IL-10 and integrin signaling pathways are associated with head and neck cancer progression. *BMC Genomics* 2016; 17: 38.
- [28] Cerami E, Gao J, Dogrusoz U, Gross BE, Sumer SO, Aksoy BA, Jacobsen A, Byrne CJ, Heuer ML, Larsson E, Antipin Y, Reva B, Goldberg AP, Sander C and Schultz N. The cBio cancer genomics portal: an open platform for exploring multidimensional cancer genomics data. *Cancer Discov* 2012; 2: 401-404.
- [29] Gao J, Aksoy BA, Dogrusoz U, Dresdner G, Gross B, Sumer SO, Sun Y, Jacobsen A, Sinha R, Larsson E, Cerami E, Sander C and Schultz N. Integrative analysis of complex cancer genomics and clinical profiles using the cBioPortal. *Sci Signal* 2013; 6: p11.
- [30] Bergmann JH and Spector DL. Long non-coding RNAs: modulators of nuclear structure and function. *Curr Opin Cell Biol* 2014; 26: 10-18.
- [31] Zequn N, Xuemei Z, Wei L, Zongjuan M, Yujie Z, Yanli H, Yuping Z, Xia M, Wei W, Wenjing D, Na F and Shuanying Y. The role and potential mechanisms of LncRNA-TATDN1 on metastasis and invasion of non-small cell lung cancer. *Oncotarget* 2016; 7: 18219-28.
- [32] Li P, Zhang G, Li J, Yang R, Chen S, Wu S, Zhang F, Bai Y, Zhao H, Wang Y, Dun S, Chen X, Sun Q and Zhao G. Long Noncoding RNA RGMB-AS1 Indicates a Poor Prognosis and Modulates Cell Proliferation, Migration and Invasion in Lung Adenocarcinoma. *PLoS One* 2016; 11: e0150790.
- [33] Guo F, Guo L, Li Y, Zhou Q and Li Z. MALAT1 is an oncogenic long non-coding RNA associated with tumor invasion in non-small cell lung cancer regulated by DNA methylation. *Int J Clin Exp Pathol* 2015; 8: 15903-15910.
- [34] Lu L, Xu H, Luo F, Liu X, Lu X, Yang Q, Xue J, Chen C, Shi L and Liu Q. Epigenetic silencing of miR-218 by the lncRNA CCAT1, acting via BMI1, promotes an altered cell cycle transition in the malignant transformation of HBE cells induced by cigarette smoke extract. *Toxicol Appl Pharmacol* 2016; 304: 30-41.
- [35] Nie W, Ge HJ, Yang XQ, Sun X, Huang H, Tao X, Chen WS and Li B. LncRNA-UCA1 exerts oncogenic functions in non-small cell lung cancer by targeting miR-193a-3p. *Cancer Lett* 2016; 371: 99-106.
- [36] Richards EJ, Permuth-Wey J, Li Y, Chen YA, Coppola D, Reid BM, Lin HY, Teer JK, Berchuck A, Birrer MJ, Lawrenson K, Monteiro AN, Schildkraut JM, Goode EL, Gayther SA, Sellers TA and Cheng JQ. A functional variant in HOXA11-AS, a novel long non-coding RNA, inhibits the oncogenic phenotype of epithelial ovarian cancer. *Oncotarget* 2015; 6: 34745-34757.
- [37] Wang Q, Zhang J, Liu Y, Zhang W, Zhou J, Duan R, Pu P, Kang C and Han L. A novel cell cycle-associated lncRNA, HOXA11-AS, is transcribed from the 5-prime end of the HOXA transcript and is a biomarker of progression in glioma. *Cancer Lett* 2016; 373: 251-259.
- [38] Jiang W, Tian Y, Jiang S, Liu S, Zhao X and Tian D. MicroRNA-376c suppresses non-small-cell

- lung cancer cell growth and invasion by targeting LRH-1-mediated Wnt signaling pathway. *Biochem Biophys Res Commun* 2016; 473: 980-986.
- [39] Su J, Wu S, Wu H, Li L and Guo T. CD44 is functionally crucial for driving lung cancer stem cells metastasis through Wnt/beta-catenin-FoxM1-Twist signaling. *Mol Carcinog* 2015; [Epub ahead of print].
- [40] Tong Y, Liu Y, Zheng H, Zheng L, Liu W, Wu J, Ou R, Zhang G, Li F, Hu M, Liu Z and Lu L. Artemisinin and its derivatives can significantly inhibit lung tumorigenesis and tumor metastasis through Wnt/beta-catenin signaling. *Oncotarget* 2016; 7: 31413-28.

# Prospective target gene network of key miRNAs Influenced by HOXA11-AS

**Supplementary Table 1.** Potential target genes of 10 miRNAs in NSCLC

CCND2	NDUFB5	HMG2	GTPBP10	HNF4A	RASSF8	OSGEPL1	PPP1R12B	ELL2
RTKN2	NXPH1	UNC80	PAFAH1B2	DGCR6	IDE	PSTPIP2	RDH11	BCAT1
ATP1B2	ATAD1	AP1AR	TRAF1	PPP1R16B	SBN01	DHFRL1	PKN2	THAP6
SOC57	G6PC2	COBLL1	HJURP	RADIL	ACSL4	PPP1R2	CNIH3	LHX9
WSB1	B4GALT4	ARHGAP28	AAED1	DAP	C10orf32	QTRTD1	FBXO32	ANKRD6
IBA57	ATP9A	KSR2	IRGQ	C2orf50	PHLPP2	CHD5	KIAA1919	NR4A3
CRKL	CSMD1	ABCD3	NDUFS5	ERN1	CRLS1	JAK1	THTPA	OTUB2
RAB8B	MMP24	C5orf24	EXOSC6	NF2	NUP62CL	FAM208A	C1orf210	AMOTL2
C17orf85	CACNA1C	ALCAM	UBXN2A	POM121	REST	CASP2	DLEU7	HELZ
BICD2	SH3TC2	BAG4	RNF169	TRIM25	FEM1B	GTF2H3	DIP2A	TMEM132D
GOLGA1	ARIH2	ZNF704	ADIPOQ	HEYL	VAPB	GATM	RAD23B	C2orf88
PLAGL2	GOLGA3	CARD8	AC023632.1	URM1	ADH7	PDHA1	MAOA	DTNA
WWTR1	EVC2	FOXN2	ANKRD34C	CENPM	HIGD1A	RNF38	MED14	TBC1D12
TCF4	DGKG	FBXO21	C7orf55-LUC7L2	ZNRF1	FAM86C1	PAK1	RPRD1B	TCF12
UBN2	TNPO1	KLF7	CHSY1	TMEM239	SLC10A2	GIMAP1	ASAH1	EDIL3
LANCL3	NDFIP1	BEND4	TNKS	VPS33A	RAN	SORT1	FKN	COL4A4
SDC2	KCND3	DNAJC27	LRP10	LAX1	CREB5	ZNF605	SLAMF6	GOLGA4
PANK3	PAIP2B	KLHL28	PITPNB	C10orf67	ANGPT2	SLC35F1	ELK4	NAV2
TENM1	GXYLT1	GPAM	KLHL2	EMP2	DNM3	NRGN	METTL6	OPCML
EML6	PHF12	MECOM	PPP1R9A	NOP9	BCL2L11	NUAK2	AFAP1	TMEM167B
FAM168B	ALKBH5	MKX	TCF7L1	VASH1	NFIB	TC2N	ZFP36L1	BCOR
SLC35E2B	TNFAIP1	INTU	SMAD7	HPS4	IRF5	SETD2	NABP1	EDDM3A
FKBP5	SNX1	DDX6	TMEM41B	DGKD	TGOLN2	CYLC2	GNB1	LARP4B
DDIT4L	KIF21B	DDX3X	EPG5	IQSEC2	TMEM231	BPTF	RSF1	CISH
CCDC38	UBE2G1	TEX15	ZNF557	ANKRD52	NPY2R	SLC7A5	AC107021.1	SNX16
DDI2	SPTBN4	PCDH18	A4GNT	ASAP2	FAM9C	ZNF69	LPPR5	CBLL1
RIMS2	TXLNA	VGLL3	CD53	RASSF4	PDSS2	CELSR1	FBXL4	GRIP1
TOR1AIP2	HIF1AN	QKI	OSBP	TMEM170A	GPA33	SMOC1	AMER2	GPATCH8
NRXN3	PRDM15	GMFB	DTWD2	ZNF442	VDAC2	VAMP3	ADD3	ELF1
HIPK1	POLR1A	AHR	DDX17	SIK2	FRMD4B	CLVS1	ENPP4	SP4
KIAA2022	CDKN2D	CD200R1	C14orf142	SPATC1	WHSC1	MLEC	ZNF230	HNRNP1
RAP2B	TPP1	CGGBP1	RBMS1	MEGF6	CD177	FAM155B	CCDC39	NRN1
CLCC1	TMEM260	SMEK1	ATAD2B	MDGA1	UQCRCQ	MSANTD2	CHD6	FAM8A1
SPAST	FBXL18	MEIS2	ARHGEF12	TMEM178B	C20orf112	FAM49B	NCEH1	ZNF624
PURB	GNAO1	ABHD2	CANX	CGNL1	PTCD2	GSTCD	TSHZ2	AGL
VPS13D	CTNND1	SMCHD1	ELMOD1	PHC1	MCF2L	C17orf105	PEX13	EIF3J
ARSB	MFSD4	SLC5A3	TOX	FLCN	VPS26B	PLXNA4	ZCCHC3	PDHX
STX7	GAS7	VKORC1L1	SYNE2	ICMT	C6orf89	EXD1	PDIK1L	ZNF730
PAK1IP1	TNS3	GABRB3	KIAA1107	CSMD2	CTNNA1	CHP1	SERINC5	ZDHHC21
CCNY	ABR	FAM169A	ITGB3	NCKAP1L	TTL	ZNF445	ANKRD29	RBM41
UBE2D3	NOS1	SRSF1	ETNK1	PDE7A	D2HGDH	CHMP5	MLLT10	NXPE3
ZNF451	WNK3	CYLD	GPR61	CALN1	ATG12	DOCK8	PHF13	NDUFA5
LIN28B	NFATC2	EIF4E3	RAB33B	PTPRN	SLC30A3	ATP11A	FOXO3	ZDHHC2
LNPEP	VANGL1	NRARP	FAM73A	TMED10	LBH	TRPV2	NAALAD2	SFPQ
ARL5B	TMEM2	MET	L2HGDH	PTPLB	ZNF592	C2CD2	FAM214A	PELO
THAP2	AR	MMP16	TTC13	ENTPD1	GPC6	ZNF12	DCLK3	N4BP2
RSBN1	AGO2	PDE5A	TMEM248	CASP9	LANCL2	SPN	RABGEF1	OXCT1
RNF152	SLC30A7	ANKS1B	SEPHS1	NPY4R	ANKRD17	MARK1	IMPACT	CHL1
PLEKHA8	RALGAPB	CCPG1	WDR26	ADAM11	FEM1C	MTPAP	SLC7A11	SEN6
TAOK1	ACSBG1	FLVCR1	TSPAN3	GIGYF1	YAE1D1	TBC1D13	GLCE	ABI3BP
TARDBP	PLEKHG4B	ONECUT2	SLC4A7	APC2	NUDCD3	KIF1C	GFPT1	RIMKLB
IKZF2	ATP8A2	COX15	BMPR2	MLXIP	AGPAT5	MUC21	MAPK1	STYX
YWHAZ	FNBP1	SF3A3	HAPLN1	ANKS1A	DPYSL2	ZHX3	RAB3GAP2	ELMOD2
EIF1AX	HEG1	OPA3	KLHL9	FBXL12	PHOX2B	HS2ST1	GLB1	TYW3
SV2B	EXPH5	NBP16	PDGFD	KCND1	AGO4	HP1BP3	RCBTB1	NUS1



## Prospective target gene network of key miRNAs Influenced by HOXA11-AS

G3BP1	KIAA1549	GK5	RUNX1T1	RASL10B	KIAA1407	HUS1	ZBTB34	SASS6
ERLIN1	FOXP1	BSDC1	TFAM	RAI14	CCDC93	ARHGEF26	HAO1	FAR1
MBNL3	SH3PXD2A	ELL	RBFOX2	PLCB3	KIAA0947	TLK1	ADAMTS9	BTN3A3
KLF11	KIAA0513	ELP6	NBN	DCTN3	UBR7	FAM160B1	CAMK2D	SMIM14
SLC45A4	CEP63	C1orf158	LIN54	RGAG4	BAHD1	ATP6V0A2	PPIG	SYNPR
FZD4	MPP2	NHS	TRABD2A	TOM1L2	ATG9A	ANKRD40	CFHR4	IER3IP1
SATB2	MEF2D	DRAXIN	PAX3	FEM1A	FARP1	CBLN2	PCYOX1	PTP4A1
XPO4	CASP10	RD3	APBB2	SPEN	RELL1	CCDC117	CLTC	ZNF131
ZFHx4	CBL	EGFLAM	LHFPL2	ZNF101	MICA	DDI1	PPARA	GHR
PLAG1	ZFYVE26	ZSWIM6	SNX6	NR6A1	NOTCH2	NCAM2	VCCKMT	CEP170
APPL1	TMEM109	KRI1	IMPAD1	AGFG2	CHCHD5	PALMD	RORA	SUV39H2
TMEM236	NCR3LG1	GMPPB	RP5-105215.2	SPECC1	NMT1	USP33	MICAL3	UBXN7
PTPRN2	RNF111	TNS4	AVL9	MTMR10	DUS1L	ADH4	DLGAP2	MAP1LC3B
CBX5	SP1	MAP9	PHAX	KIAA1875	HOGA1	TMEM243	SS18L1	IL13RA1
ZNF772	TET2	CAMKK2	PURA	COA1	IL17RB	HAUS3	ST8SIA4	NTS
RPS6KA3	MSRB3	AMZ1	NAP1L5	FAM60A	EGLN3	DPPA4	KIAA0408	ZC3H12C
ZNF148	RAG1	USP47	PPP1CB	PDE2A	TENM4	LYRM7	SGIP1	PRNT
SLC16A6	PALM2-AKAP2	ZNF576	INTS2	SHISA6	TEDDM1	AAK1	MTUS1	TUSC3
MCU	UBE2H	ANO10	UNC5D	ADM2	HLA-DPB1	UTP15	NUDT11	GRID2
SLC44A1	PLCG1	PLEKHO2	SV2A	NLRC5	MRE11A	LBR	ITPRIP	COL4A1
BZW1	CNTF	SASH1	ZHX1	PEA15	SS18	AP1G1	EDAR	RBM39
BRWD1	EHD3	SORCS3	ADSS	KREMEN1	HECTD3	PTPLAD1	MEGF9	TOMM20
WHSC1L1	C17orf51	EYA3	FAM13B	AC008060.7	FAT3	HBEGF	KIAA0040	CNOT4
MFHAS1	SIPA1L2	RAB1A	SLC4A4	TTYH2	STK35	PRRG4	LSM11	KRAS
RC3H1	ZNF80	GFRA1	ZADH2	TSPAN9	DNAJC13	IREB2	KAT6B	LEPROT
C1orf21	KIAA1456	SOS1	ABL2	QSOX1	PHF20	PRR14L	CWC25	LMBRD2
LPP	MECP2	SYNRG	YIPF4	CYB561D1	OSTN	SCD	CD28	ZFP30
AMER1	CPEB3	TMC01	ZBTB38	FAM131B	FBXL17	CRISPLD1	ADNP	TXNL1
CA13	LCOR	RAD51	ITGA1	PARD3B	GPR107	SFMBT2	MYO6	GOPC
AK3	KIF5C	FRS2	PRKAA1	ETV6	MED8	CNEP1R1	ZNF37A	SYT1
LRAT	MYT1L	NOVA1	ZNF595	LRRC14	CHTF8	DSPP	NFATC3	ZNF302
NRAS	SCN7A	CLDN11	STC1	GGA2	NAA40	RGS5	C5orf63	SEMA3D
KMT2A	CCSER1	EXOC8	ANK2	ZNF562	SUZ12	SNPH	RORB	ARID4A
EBF3	TTLL7	CNTNAP2	USP45	PSMF1	CDH2	CUL5	STXBP5L	ALKBH8
TFEC	MON2	CTPS2	DOK6	LPPR4	LMAN1	ZFAND3	PRPF38A	HNRNPH2
EXOC5	CCDC6	FBNP1L	CACNB4	PODXL	NRXN1	RASAL2	REL	DPY19L1
LDLRAD2	S1PR3	TSPAN31	INPP4B	TBC1D16	CDK13	ZMIZ1	LRRFIP2	ZNF347
CYB5B	SIX4	OR51E2	UBL3	NUDT8	SRGAP1	ZBTB44	TLL1	COMMD2
SLC24A4	DST	MTSS1	ENTPD4	DNPEP	ZNF703	MAK	GDA	MTF1
SNX22	PDS5A	LY6K	PDZD8	RFFL	TCF7L2	RBM43	LRRN1	APP
SLC25A45	HEY2	SIGLEC8	NRIP3	LZTS2	PGM2L1	ZNF638	DCAF4L1	BCLAF1
STX6	FAM217B	PPP1R15B	FAM133A	CAMK2G	EFNA5	RAB2A	POF1B	ZNF548
ZNF783	SOX11	NUTM2G	ATP6V0D2	B3GALT4	F2R	BTN3A1	LZTFL1	MACC1
URB1	MXRA5	TPM3	RAB11A	AP3M1	FBXO38	SMAD9	PAWR	RB1
RNF165	TSPAN14	LIMD1	SREK1	USB1	LYRM2	PALM2	FAM49A	RPRD2
UBE2R2	PIGN	CXorf56	RLIM	RSRC2	SLCO4C1	TMEM33	PTPN4	SERPINE1
ORAI2	RAB27A	THAP1	TMEM168	DHX35	SAMD4A	HLF	SETBP1	GAB1
NPLOC4	JAKMIP2	ITSN1	ATP2B1	PCGF3	KBTBD8	ASH1L	AHCTF1	ABRA
ELMSAN1	LONRF2	TMEM241	RIN2	TBCEL	MMGT1	TSPYL5	AC011294.3	OSBPL8
GNB1L	KCNK10	C6orf141	OTUD4	PLGLB1	ZNF441	SNX29	ZC3H14	ANO5
NBPFF20	DIP2C	OIP5	WNT3	ADARB2	CHORDC1	SSBP2	USP38	FAM204A
GLUL	CEP57	C2orf48	C1orf141	LETMD1	DNAJC15	VWC2L	THSD7A	IDS
DHODH	INO80D	OGFRL1	FRYL	SLC6A4	FOXG1	NUCKS1	FAM19A2	PPARGC1A
CACNB2	PDE4D	MDM2	PPP1R12A	TTYH3	DUSP3	FTO	DZIP1	PAQR3
HRK	RNF11	NDRG1	TMEM185B	STIM1	NLK	MS4A4A	TBL1XR1	SERP1
PLXND1	TIA1	RPL28	GNG2	GIT1	NETO1	NECAP1	MT01	NF1

## Prospective target gene network of key miRNAs Influenced by HOXA11-AS

MED13L	HSPA4	IPCEF1	UBE2K	MREG	SPATA18	SLC35D1	CHIC1	C2orf69
FAM110B	C11orf30	TMEM167A	FRMD4A	UBE2N	TMEM133	MAPRE2	FGF13	CCNA2
CSNK2A1	SCRN1	SLC16A4	HMGCR	POP4	ZNF776	LRRC8B	ITCH	MAN1A1
SMC1A	TP53INP2	NR2F6	ZFP62	KIAA1429	TMEM206	NCOA2	MAF	ZBTB21
KIAA0232	SCML2	RP11-664D7.4	IL17RD	KMT2D	XRCC2	KLF13	FPR2	PTPRG
GPCPD1	CDC73	TAF8	RHOU	RAD9B	ANKRD34B	ERGIC2	SOC5	SLC30A1
FBX045	CACYBP	SHANK2	PHACTR2	CDON	CCDC141	SYAP1	ATRNL1	PGR
HTR7	FIGN	LY6G5B	UTP6	LIN28A	TMEM30B	DERL3	PSPC1	PEG3
MED13	ZNF793	FAM124A	SLC25A36	DNAJB14	BORA	WASL	COL11A1	KIF3A
CYFIP2	WWC3	DTD2	ADAMTS3	ARID1A	ZNF641	GK	SLIT2	TMEM50A
GPATCH2L	CREB1	ADAT1	SPRY4	ARHGAP17	NAA50	GGA3	BNC2	SH3RF1
MGA	TFAP2B	SHOX	AKAP11	MBTPS1	CDYL2	SFR1	SESTD1	VAMP7
SYT11	CXorf57	MINOS1	MRPS35	TOR1B	SF3B1	MAGI3	SRSF12	STMN2
GXYLT2	SLC16A14	KIAA1462	KIAA1549L	IVNS1ABP	SPRY3	SIGLEC14	ATRX	HNRNPU
CACNG8	FAM126B	HSF5	STK38L	SLC6A5	TLR4	RAB6B	MNAT1	GULP1
ENPP1	YY1	IFNAR2	TMTC3	TNIP3	HERC4	IRAK3	ATXN7L1	MLLT4
NTRK2	AK2	GPR75	GZF1	ENTPD3	ANKIB1	FAM53C	PGRMC2	MAP3K5
ANKRD28	LRP6	WDR73	VEZF1	PLD1	PPP2R5E	RBM46	FAM102B	MED10
RAB13	CEP78	DARS2	ZYG11B	FAM78A	WAC	MARCKS	ZNF721	GPR64
UBE2J1	SORBS1	PHKG2	PCF11	PSEN2	KLHL24	BRIP1	SNRPF	LEMD3
ARL6IP5	MTMR12	NFATC4	UBA6	TSC1	NDUFAF4	CLCN5	ATP2C1	CREBL2
MFS6	MTMR7	TMEM127	TMEM170B	STS	ARF6	CEP97	PCNX	TBL1X
MIER3	KIAA1958	RHD	CAB39	ZFAND5	A1CF	RECK	PIK3C2A	ARHGAP18
ESRRG	RBM12B	ZNF581	RSAD2	SRPR	SPRYD7	STEAP2	PRPF4B	FAM198B
METTL20	AFF2	PACS2	KCTD16	HSPA12A	PWWP2A	SLC30A6	FZD7	IBTK
RNF217	KLHL31	PLEKHG2	RBM27	AGFG1	GPR155	TRIM44	PPP2R5C	CCDC144NL
STEAP4	NCOA7	TAPBP	SALL3	RAB11FIP2	CCNT1	FAM26E	WDR36	DPP8
RHOT1	PIK3CB	GRSF1	USP6NL	TEF	TFAP2A	FGFR10P	TGFB1	PRSS16
ZNF681	RAP1A	ZNF566	GCLM	GALNTL6	PBX2	ZNF708	SLC30A4	RNF212
PPEF2	PRKAA2	EIF2S3	BBS4	ALDH8A1	RASSF3	KLHDC10	KLHL4	USP22
CASC4	PAPD5	ADAMTS4	MKL2	ETFA	ZNF197	CYP26B1	LCA5	STMN4
MLH1	TRIM33	APAF1	CSRNP3	UBN1	NUDT7	ZNF100	UBE2B	UBE2V2
SOAT1	PHF3	PDPN	USP31	ESRP1	FGF20	FAM227A	GABPA	FAM63B
ZMYM1	JMJD1C	PGAM5	NIPA1	RNF41	ZCCHC24	CDK19	GLRA3	KRTAP19-1
ZC3H6	ZDHHC15	H2AFJ	ZNF649	GLYCTK	DEPTOR	PPP1R1C	ZCCHC14	EDNRA
SHOC2	FRK	PATZ1	EXTL2	AGO1	PEX11A	LMX1B	DIP2B	PKHD1
HPSE	EPHA7	MRPL49	PCDH17	TRPS1	SEMA5A	ST8SIA2	HNRNPF	SCN3A
BVES	BCL11B	C10orf111	TXNDC15	KPNA6	MVK	FAM160A1	GTPBP4	PAX1
APOL6	LUZP1	CYP2B6	GABPB2	ADAM12	C2orf68	NCOA4	SLC9A6	COL8A1
NMNAT2	SLC25A44	ZNF490	SNAP25	LRRK2	OXR1	ZSWIM1	DCUN1D1	FBX030
SYDE2	EXT1	SYTL3	MMACHC	PICALM	CDK5R2	MAP3K3	HNRNPDL	CREM
TSPYL1	ZNF264	CDKAL1	RASSF6	SH3BGR2	PPM1E	ZNF709	JAM2	HNRNPDL
ZBTB8B	XPNPEP3	TMED4	ECE1	VASH2	COPS2	UBE2QL1	LRRC7	TMEM68
TVP23C	C20orf197	MDM4	TSN	FRAT1	SMYD1	PABPN1	ZNF280B	TSPAN12
RASEF	ADRBK1	UBB	DHX38	FAM149B1	FAM182B	FOXN3	FBXW11	SPPL2A
TMEM209	NCOR1	ANKS4B	NQO1	SPIRE1	CNTN2	SZT2	PCDH9	YRDC
TRIM2	PIP5K1C	C3	FRMPD3	HIC2	CIITA	SNX11	ARHGEF33	MB21D2
CBFA2T2	KIAA0226	GJB1	NAA15	TMX4	PSD2	ADAR	CDC42SE2	UBE3A
GNS	KPNA1	ZNF583	ZNF423	TCEANC2	GSK3B	MAP3K9	MEX3C	COX7C
CTTNBP2NL	MAP1B	ZNF891	FAM71F2	STK25	IL36RN	ALDH4A1	DHX36	TP53RK
CASP16	EP300	CCDC77	AMOT	CDK8	GOLGA6L1	RP11-863K10.7	DAAM1	SATB1
LIFR	TM9SF3	PSMC4	FAM222B	GCC2	PDGFRA	SKAP1	MITF	USP27X
NUP43	RAB14	GALNT2	PIP4K2C	EXOC2	CCNF	SPOCK2	TTC37	DCAF17
PDP2	EIF5A2	AQP6	RAPGEF6	CDK17	RBM23	NOS1AP	DKK2	AFF1
MBOAT2	CREBZF	BROX	NOA1	IL6R	DGKB	NKAIN2	DARS	CCDC50
ZDBF2	DCP2	WNT1	NAT8L	KLHL7	DCAF7	SETD7	HECTD2	C5orf15

## Prospective target gene network of key miRNAs Influenced by HOXA11-AS

RPL37A	SYNJ1	SIKE1	NAALADL1	BDP1	C16orf74	RABL2A	BAMBI	CCDC108
MARVELD2	ULK2	ZNF528	STRIP1	MKLN1	DGKI	MOAP1	C5orf47	CACNA1B
GPR158	TNRC6B	BPNT1	TRAM2	HHIPL1	HAAO	ABCA12	ZFPM2	RAB21
AKAP12	EFCAB11	NHLRC2	NAB2	WDPCP	HEMK1	CASQ1	CREBBP	GUCY1B3
PTGER3	CADM2	RNASEH2B	EMR2	MAN1A2	KPRP	CELF2	CTNNB1	TPRXL
CLDN12	AKR1C2	AC008394.1	NAA60	SLIT1	TMEM92	SLC29A1	REPS2	NPR3
HELLS	THUMPD1	MRPS16	UNC119B	GFOD1	DPF2	ABHD17B	BMP2	INHBB
SERBP1	ACAP2	SSR1	SH3BP2	ACOT11	ALDH6A1	RABL2B	IRS2	PDCD10
SLC16A10	ATXN3	CD209	FAM203A	FAHD2A	SLC25A34	CYP8B1	CHST2	PLCL1
STRN	GTF3C4	GDE1	MXRA7	MBTD1	PGGT1B	SLC23A2	ARHGAP20	ABI1
ZNF543	ZNF555	LZIC	ZNRF3	NUMB	C3orf70	TMEM18	EMC2	ELOVL6
MYO5A	USP15	AGBL5	TAL1	CLCN3	LIX1L	MAP2K6	FNIP2	RANBP2
ZNF652	RAB22A	ORC4	ARL5C	SOX6	KLHDC8A	FSTL4	G3BP2	NRG1
FBXL5	CA5B	INADL	GRIK3	PIK3R1	SOGA1	CLASP2	PGAP1	WAPAL
ST6GALNAC3	THSD4	ZNF850	MAP3K4	LIN7C	TRIM66	FOKK1	CPSF6	H3F3B
XRN1	PLXDC1	SPC24	CCDC85C	PTCHD1	BLCAP	MSL2	PCMTD1	GGCX
FZD3	CTNND2	AS3MT	TSPEAR	BTAF1	GOLGA6L6	PRIM1	GSPT1	INSIG1
PHKB	GLI3	CD3EAP	CCBE1	KIFAP3	SLC7A1	PITPNM3	RAD51AP1	ATXN1L
RNF138	CCDC68	MYADM	C10orf105	SLC15A4	CD47	SYT17	TXLNB	TEAD1
CNOT6L	SMC5	CLPB	LRRC27	DYNC1LI2	EIF1AD	SERINC1	RRP15	PSD3
LUC7L3	PIP4K2A	C5orf45	PDE1B	TMEM132C	TAF5L	ITPKC	CAAP1	NTRK3
B4GALT5	SNRPD1	UGGT1	KRBA1	CACUL1	EIF3B	TAPT1	IKZF5	NPAS3
DHX40	ZEB1	SFXN2	TMEM110	SIPA1L1	C6orf223	FIBCD1	ABCA1	ITPR2
PRKX	PPP1R3D	MAB21L3	TRIM62	TGM3	AQP10	MFRP	PAPPA	EIF2AK2
TBCA	AP1S3	KLHL23	NBPF24	MVB12B	CSF1	FOXP4	METTL15	ZNF800
SRSF2	KLF6	ZNF141	C17orf103	TPRX1	DTX3L	SLC43A2	FBXO33	MAPK8
ZMYM4	FAM210A	SLC8A3	C17orf70	DFFA	CHRNA4	TFCP2L1	PPP1CC	PTEN
ANTXR2	SAR1B	ZNF665	USP20	DSC3	ABHD15	PLLP	ITGAV	ANP32E
DYNC111	KIAA2018	GPI	FAM203B	ZNF662	UBXN2B	RGPD2	SULT2A1	WDFY3
MXD1	KIAA0355	ZNF716	SLC12A6	STX16	MAZ	TRIM24	NOX4	BRWD3
RSRC1	DPY19L3	ZNF585B	WTIP	PEG10	IL2RB	CPEB4	NAPEPLD	NFAT5
SLC35F5	BAALC	CARD6	LZTS1	RFX7	GALNT16	DIO2	TFRC	ADAM22
RNF222	SPRED1	SLC27A1	DPYSL5	MTMR11	NDRG3	RNMT	EPC1	FXR1
ERBB4	BAZ2A	ARL10	TBC1D20	MESDC2	IGSF3	BMPR1A	CSNK1A1	CREBRF
KHDRBS2	MOB1B	SARM1	MYO18A	PIKFYVE	CHMP1B	NIPSNAP3A	ZNF292	SYNCRIP
CLDN1	ZNF440	PDPK1	C7orf65	ERLIN2	DCUN1D5	RNF144B	SPIN1	ATXN7
TMEM192	SLC44A5	FAM212B	HEATR1	NIPBL	TRMT6	ZNF460	SEMA6A	AFF4
SEMA3E	CUL3	CAMLG	PLCXD1	SLC38A4	RAVER1	TMEM106B	SAP30L	UBE2W
SESN3	SOCS4	PER2	KCNH8	IL1RL2	PLEKHG5	CXADR	MYLIP	POU2F1
CDKN2AIP	C5orf51	RPH3AL	SNX27	AMMECR1	SFT2D2	RPP14	FAM46A	DICER1
NFIA	CAMSAP2	RAB36	PREB	NEDD4L	NUFIP2	TP53	HOMER1	ZNF770
NCAM1	SYNM	TXNDC16	PDDC1	C17orf80	TFDP2	GTF2A1	SAP18	SLITRK4
ZNF726	KLF12	BTF3L4	ZSCAN25	VEZT	KATNAL1	USP24	HDAC2	HIPK3
SPRY1	MSANTD3-TMEFF1	UBA52	SMG5	FAM91A1	CS	CPSF7	TGFA	
TTC14	TMEFF1	ZNF674	ANK1	ZBTB24	TCP11L1	C14orf105	GABRA4	
RNF145	DCAF5	LHX6	PPM1L	HNRNPA2B1	TRIM26	OSTM1	GGNBP2	